MOLECULAR ECOLOGY

Molecular Ecology (2015) **24**, 5910–5926 doi: 10.1111/mec.13425

Speciation processes in putative island endemic sister bat species: false impressions from mitochondrial DNA and microsatellite data

HAO-CHIH KUO,* SHIANG-FAN CHEN,† YIN-PING FANG,‡ JAMES A. COTTON,*[1] JOE D. PARKER,* GÁBOR CSORBA,§ BURTON K. LIM,¶ JUDITH L. EGER,¶ CHIA-HONG CHEN,** CHENG-HAN CHOU†† and STEPHEN J. ROSSITER*

*School of Biological and Chemical Sciences, Queen Mary University of London, London E1 4NS, UK, †Center for General Education, National Taipei University, New Taipei City 23741, Taiwan, ‡Department of Biological Resources, National Chiayi University, Chiayi City 60004, Taiwan, §Department of Zoology, Hungarian Natural History Museum, 1088 Budapest, Hungary, ¶Department of Natural History, Royal Ontario Museum, Toronto, ON M5S 2C6, Canada, **Shei-Pa National Park Headquarters, Miaoli County 36443, Taiwan, ††Division of Zoology, Endemic Species Research Institute, Nantou County 552, Taiwan

Abstract

Cases of geographically restricted co-occurring sister taxa are rare and may point to potential divergence with gene flow. The two bat species *Murina gracilis* and *Murina recondita* are both endemic to Taiwan and are putative sister species. To test for nonallopatric divergence and gene flow in these taxa, we generated sequences using Sanger and next-generation sequencing, and combined these with microsatellite data for coalescent-based analyses. MtDNA phylogenies supported the reciprocally monophyletic sister relationship between *M. gracilis* and *M. recondita*; however, clustering of microsatellite genotypes revealed several cases of species admixture suggesting possible introgression. Sequencing of microsatellite flanking regions revealed that admixture signatures stemmed from microsatellite allele homoplasy rather than recent introgressive hybridization, and also uncovered an unexpected sister relationship between *M. recondita* and the continental species *Murina eleryi*, to the exclusion of *M. gracilis*. To dissect the basis of these conflicts between ncDNA and mtDNA, we analysed sequences from 10 anonymous ncDNA loci with *BEAST and isolation-with-migration and found two distinct clades of *M. eleryi*, one of which was sister to *M. recondita*. We conclude that Taiwan was colonized by the ancestor of *M. gracilis* first, followed by the ancestor of *M. recondita* after a period of allopatric divergence. After colonization, the mitochondrial genome of *M. recondita* was replaced by that of the resident *M. gracilis*. This study illustrates how apparent signatures of sympatric divergence can arise from complex histories of allopatric divergence, colonization and hybridization, thus highlighting the need for rigorous analyses to distinguish between such scenarios.

Keywords: gene flow, introgressive hybridization, *Murina*, nonallopatric divergence, Taiwan

Received 7 July 2015; revision accepted 13 October 2015

Correspondence: Stephen J. Rossiter,
E-mail: s.j.rossiter@qmul.ac.uk
[1]Present address: Wellcome Trust Sanger Institute, Wellcome Trust Genome Campus, Cambridgeshire CB10 1SA, UK

Introduction

The expectation that drift and selection will more easily establish genetic differentiation between populations with little or no gene flow has led to the overwhelming view that most cases of speciation must involve a period of geographical isolation (e.g. Barraclough & Vogler

2000; Turelli *et al.* 2001). Despite this, theoretical models have proposed routes by which parapatric and sympatric speciation (hereafter collectively referred to as 'nonallopatric speciation') can proceed (Slatkin 1982; Rice 1984; Dieckmann & Doebeli 1999; Gavrilets & Waxman 2002) and these studies have been complemented by several empirical examples that suggest nonallopatric speciation could be more common in nature than was previously assumed (reviewed in Via 2001).

In evaluating potential cases of nonallopatric speciation, several researchers have advocated using biogeographical information. Lynch (1989) proposed that range overlap and relative range sizes of sister species or supra-specific taxa could be used to infer geographical modes of speciation, with substantial overlap pointing to sympatric speciation, and little overlap indicating allopatric speciation. Such reasoning has been used to argue for greater frequencies of sympatric speciation in nature than previously thought (e.g. Mattern & McLennan 2000), but has also received criticism given that a key assumption—that geographical ranges of natural organisms are constant through time—is probably seldom true (reviewed in Losos & Glor 2003; Coyne 2007).

Extending the logic of studying range overlap, Coyne & Price (2000) emphasized the value of looking for 'sister species' (species that are each other's closest relatives) that are both vagile yet restricted geographically to the same small area, such as an oceanic island (also see White 1978). Under these conditions, they suggested that sympatric rather than allopatric divergence is a likely explanation for such overlapping ranges. Coyne & Price (2000) searched for oceanic islands (area 0.8–3500 km^2) on which at least one endemic bird species occurred. By assessing whether or not each taxon's sister species coexisted on the same island or archipelago, consistent with in situ divergence, they found no clear evidence supporting nonallopatric speciation in the species pairs studied. Kisel & Barraclough (2010) extended this approach to diverse taxa and found that potential cases of in situ speciation in highly mobile animals such as moths and mammals were associated with larger island areas (approximately 140 000 and 420 000 km^2, respectively), while smaller areas were associated with possible examples from plants and less mobile animals (snails and lizards). Thus, there appears little evidence for sympatric speciation when applying Coyne & Price's (2000) criteria for island-dwelling taxa, at least for highly mobile animals.

A common criticism of focusing on geography in speciation biology is that it detracts from the underlying gene dynamics (see Hey 2006; Fitzpatrick *et al.* 2009). Indeed, it is implicitly assumed, but rarely tested, that nonallopatric divergence typically occurs in the face of gene flow, especially where reproductive isolation is thought to arise via ecological shifts (e.g. Kingston & Rossiter 2004; Jackson 2008; Forbes *et al.* 2009) rather than by postzygotic mechanisms (e.g. Husband & Sabara 2004). Recently, several empirical studies have applied newly developed isolation-with-migration (IM) models (Hey & Nielsen 2004; Hey 2010b) to demonstrate historical gene flow among closely related taxa, attributable to either nonallopatric divergence (e.g. Hey 2006; Nadachowska & Babik 2009) or, alternatively, allopatric divergence followed by secondary contact (e.g. Llopart *et al.* 2002; Geraldes *et al.* 2006). Generally, however, most such studies have been unable to date the occurrence of gene flow; simulations show that IM methods cannot provide reliable estimates of the timing of historical gene flow (Strasburg & Rieseberg 2011). Consequently, to distinguish between cases of taxa that have formed sympatrically with gene flow vs. those that evolved while geographically isolated but which have subsequently undergone secondary gene flow, additional information can be informative, including knowledge of the broader patterns of genetic affiliations with other populations and taxa, and the potential for historical range shifts in the light of climatic fluctuations.

While interpretations of speciation based on either range overlap or IM each has their respective shortcomings, these approaches are complementary and together might offer a more powerful means of testing for nonallopatric divergence. Here, we combine these methods to study the origin of two newly discovered bat species *Murina gracilis* and *Murina recondita* on Taiwan (Kuo *et al.* 2009), which phylogenetic reconstructions using mitochondrial DNA (mtDNA) indicate are sister taxa (Kuo 2004, 2013). Such cases of geographically restricted co-occurring sister species are exceptionally rare in bats; in their review, Kisel & Barraclough (2010) identified two congeneric bat species on New Zealand as the best potential example. Given that Taiwan is a much smaller island (36 000 km^2) with respect to the expected mobility of flying mammals, *M. gracilis* and *M. recondita* meet Coyne & Price's (2000) criteria and thus offer an excellent opportunity to test for nonallopatric divergence. Moreover, the fact that these taxa show contrasting altitudinal preferences, with the former tending to occur at higher elevations (Kuo 2004, 2013), further suggests the potential for ecological speciation linked to niche differentiation. We generated data sets of nuclear and mitochondrial markers for both species and applied IM-based modelling approaches alongside other population genetic analyses for gene flow at different scales. As a detailed dissection of the divergence process requires a thorough understanding of the relationship

between the two focal taxa, we also generated and analysed sequences for the continental congeneric (and also recently described) species *Murina eleryi* (Furey *et al.* 2009). We hypothesized that given their close relationship and endemic status on Taiwan, *M. gracilis* and *M. recondita* probably diverged in situ on this island and, therefore, would show evidence of a sister relationship across all markers, as well as evidence of divergence in the face of gene flow.

Materials and methods

We focused on three newly described species of tube-nosed bat from East Asia. *Murina gracilis* and *Murina recondita* are considered endemic to Taiwan (Kuo *et al.* 2009), while *Murina eleryi* has been recorded in southern China, Vietnam and Laos (Furey *et al.* 2009; Eger & Lim 2011). Sibling relationships among these three taxa have been inferred from both morphometric comparisons and mtDNA phylogenetic reconstructions, with the latter unambiguously supporting a relationship of [(*M. gracilis*, *M. recondita*), *M. eleryi*] (see Systematic notes on the focal species in Appendix S1, Supporting information). Although little is known about their respective ecologies, *M. gracilis* occurs at elevations of >1500 m above sea level (asl), whereas *M. recondita* and *M. eleryi* both occur at lower elevations of <1500 m asl (Kuo *et al.* 2014; Table S2, Supporting information).

Assessment of contemporary gene flow between Murina gracilis and Murina recondita

To test for contemporary gene flow between *M. gracilis* and *M. recondita*, we screened populations for evidence of genetic admixture using the Bayesian clustering method implemented in STRUCTURE 2.3.2 (Pritchard *et al.* 2000). Genotypes of 106 *M. gracilis* and 144 *M. recondita* at 14 microsatellite loci (A4, A9, A10, A104, A109, A118, A122, B5, B9, B114, B121, B124, D110 and D117; see Kuo *et al.* 2013) were examined under a model that assumed independent allele frequencies among genetic clusters and allowed for mixed ancestries among individuals. We ran 10 replicates of Markov chain Monte Carlo (MCMC) for between 2 and 10 clusters (*K*) with each MCMC comprising 0.75 million iterations for sampling and the same number for burn-in. To assess consistency across replicates, we used the CLUMPP procedure (Jakobsson & Rosenberg 2007) and visualized the resulting plots using DISTRUCT (Rosenberg 2004). Plots under the *K* value that best fitted the data, as justified according to the rationale proposed by Pritchard *et al.* (2000), were inspected for signatures of genetic admixture.

For each individual bat, we estimated the proportion of its genetic composition, as measured by the ancestry coefficient *q* (Pritchard *et al.* 2000), that could be assigned to its own species, summing across multiple clusters where relevant. A few individuals of *M. recondita* showed <0.9 assignment to their own species (see Results), potentially reflecting genetic introgression from *M. gracilis*. Alternatively, such signatures might arise through allele size homoplasy (SH), which can occur in microsatellites due to their hypervariable nature (Estoup *et al.* 2002). To identify those loci driving signatures of admixture, we repeated our STRUCTURE and CLUMPP analyses under the best-fitting *K* but excluded each locus one by one. Three replicate runs were conducted for each pruning scheme and, for each bat showing mixed ancestry, we recalculated *q* assigned into its own species under each pruning scheme. Loci that when pruned led to an increase in *q* (compared with values based on the full data set) were regarded as likely candidates for introgression or SH. To distinguish between these scenarios, we amplified and sequenced the corresponding flanking regions of those loci contributing most to admixture, to check for parallel signatures of introgression that would be expected under tight linkage to the simple sequence tandem repeat units. We reasoned that apparent introgression at STRs but not at the adjacent flankers would be best explained by SH.

Using the approach, we amplified and sequenced the flanking regions of two microsatellite loci (A9 and A122) in selected individuals of *M. gracilis* and *M. recondita*, including those with possible mixed species ancestries. In total, 10 bats from each of the two species were selected (indicated by arrows in Fig. 1) plus one *M. eleryi* (HNHM 2007.28.2; see Table S2, Supporting information) for comparative purposes. We designed and paired the primers A9FRL (5′-GCA ATT TCA TTG TGT CCC TTG-3′) and A9FRR (5′-GTC ATA GTT CTA GTC TCC CAG ATC C-3′) for A9, and A122FRL (5′-CAT TCT ATC TGC CTA CCT TGA CA-3′) and A122FRR (5′-GGC CTT CTC ACT AGG CAC AG-3′) for A122. PCR cocktails of 15 μL, contained 0.2 μM each primer, 2.0 μL of template, and 7.5 μL of the provided master mix of the Qiagen Type-it Microsatellite PCR Kit (QIAGEN). Reactions were performed on a Bio-Rad C1000 Thermal Cycler (BIO-RAD Laboratories) with the following thermal profile: 95 °C 5 min; 35 cycles of 95 °C 30 s, 59 °C 90 s, 72 °C 30 s; 60 °C 30 min. Sanger sequencing using primers A9FRR and A122FRR was undertaken by Eurofins MWG Operon (Ebersberg, Germany) on an ABI 3730 DNA Analyzer (Applied Biosystems).

Sequences were trimmed and the chromatograms inspected by eye for double peaks, indicative of heterozygous sites. For reads with multiple heterozygous

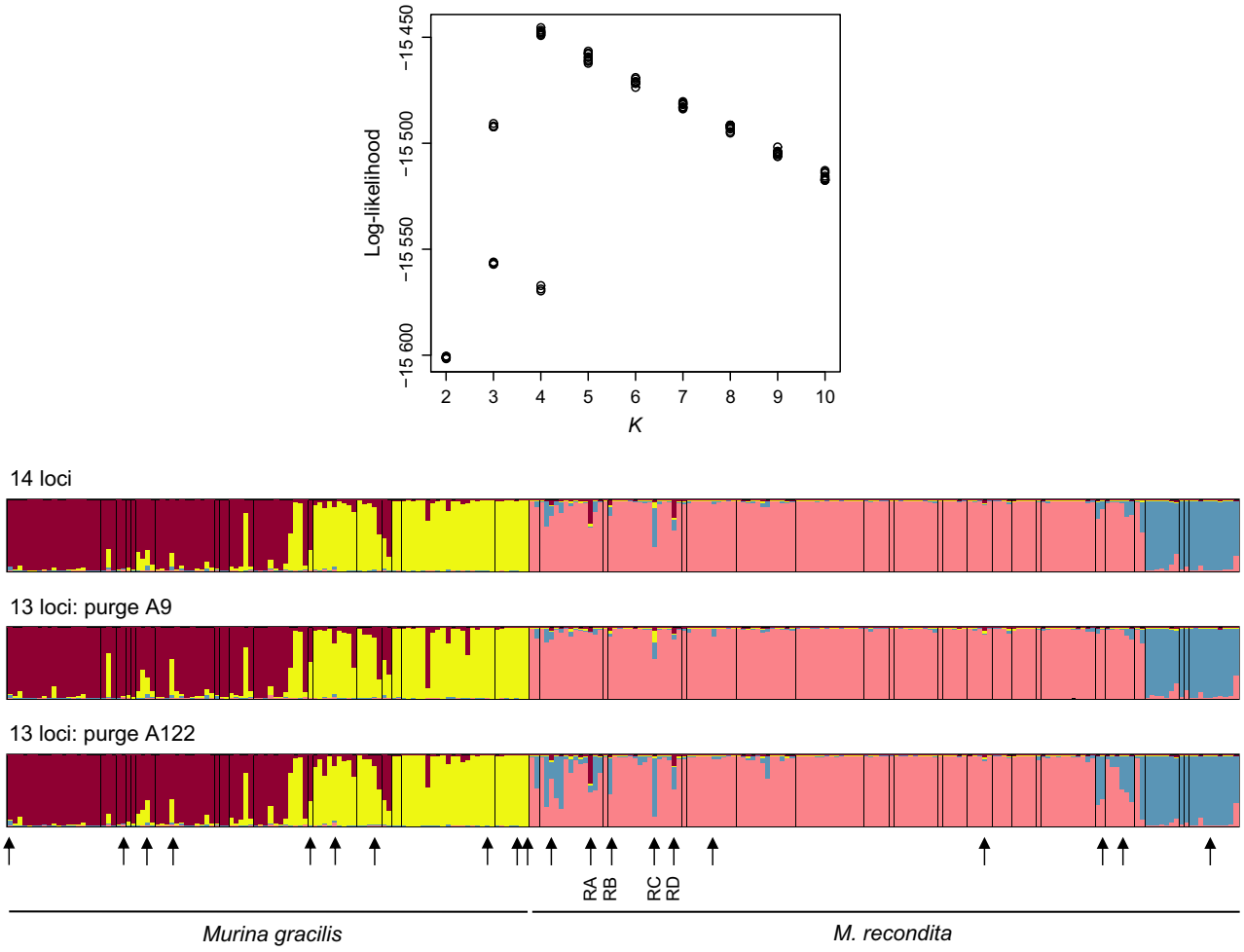

Fig. 1 Bayesian clustering analyses implemented in STRUCTURE. The upper panel shows penalized log-likelihood values (Pritchard *et al.* 2000) of 10 replicated runs under each of successive numbers of clusters (*K*) for the full data set (14 microsatellite loci). The lower panel shows DISTRUCT plots for analyses based on the full data set and based on 13 loci with either locus A9 or locus A122 removed. Selected individuals for sequencing of flanking regions of loci A9 and A122 are indicated by arrows.

sites, we used the Bayesian statistical method in PHASE 2.1.1 (Stephens *et al.* 2001; Stephens & Scheet 2005) to infer haplotypes. PHASE analysis was applied separately to *M. gracilis* and *M. recondita*, using models that both allow or disallow intragenic recombination. To facilitate phasing, known haplotypes obtained from 454 sequencing were used as references (see next section). Under each recombination model, we performed three replicated runs, each with 10 000 iterations (10 iterations per sample) following a burn-in of 1000 iterations. Haplotypes inferred by PHASE with a posterior probability of ≥0.6 were accepted (see Garrick *et al.* 2010). To investigate the segregation of haplotypes in relation to species identity, for each locus, we constructed median-joining (MJ) network using the software NETWORK 4.6.1.1 (Fluxus Technology Ltd., 2010) in which, the epsilon value was heuristically set as 10.

Divergence within the Murina gracilis complex revealed by mtDNA

To obtain a more comprehensive picture of the divergence processes among *M. gracilis*, *M. recondita* and their relatives, we further included 12 additional individuals of *M. eleryi* collected from southern China ($n = 7$) and Central Vietnam ($n = 5$) (see Table S2, Supporting information for details). Genomic DNA of these bats was extracted using the DNeasy Blood & Tissue Kit (Qiagen).

We first investigated the divergence processes based on mtDNA by expanding our earlier published data set (Kuo *et al.* 2014; see Table 1) by Sanger sequencing the partial cytochrome *b* (Cyt-*b*) and cytochrome *c* oxidase subunit 1 (COI) genes of these additional *M. eleryi* samples, which we also supplemented with published sequences (Francis *et al.* 2010; see Table 1). To infer the order of divergence among *M. gracilis*, *M. recondita* and

Table 1 Sample sizes, sources and sequencing methods (Sanger or 454-pyrosequencing) of genetic markers used for reconstruction of divergence processes among the focal taxa

	Mitochondrial markers			Nuclear markers	
Taxon	*n*	Cyt-*b*	COI	*n*	FR
Murina gracilis	87*	II* Sanger	II* Sanger	15†	I 454
Murina recondita	113*	II* Sanger	II* Sanger	15†	I 454
Murina eleryi 1‡	8	I Sanger	I, III§ Sanger	7	I Sanger
M. eleryi 2¶	5	I Sanger	I, III§ Sanger	5	I Sanger

N, sample size; FR, flanking region sequence obtained for 10 microsatellite markers; I, this study; II, Kuo *et al.* (2014); III, Francis *et al.* (2010).

*Range-wide samples for which concatenated Cyt-*b* and COI sequences are available with Dryad entry doi: 10.5061/dryad.f5th5.

†Selected samples from sites #49 and #54 for *M. gracilis* and those from sites #48, #51, #52, and #54 for *M. recondita* (see Kuo *et al.* 2014 for details of site locations).

‡*Murina eleryi* 1 refers to the single sample from North Vietnam (HNHM 2007.28.2) and samples from southern China, listed in Table S2 (Supporting information).

§Available with accession nos. HM540936-7, JQ601475, JQ601483, JQ601503 and JQ601510 for *M. eleryi* 1, and HM540933, HM540938, JQ601543 and JQ601545 for *M. eleryi* 2.

¶*Murina eleryi* 2 refers to samples from Central Vietnam, listed in Table S2 (Supporting information).

M. eleryi taxa we used Heled & Drummond's (2010) Bayesian method implemented in *BEAST. Assuming the absence of postsplit gene flow between divergent taxa, *BEAST can assess the stochastic process of coalescence by explicitly modelling effective population size along the course of divergence, and has also been shown to perform very well in estimating the order and timing of divergence events, even when applied to a single locus (see Drummond *et al.* 2012). The two mitochondrial genes were concatenated and partitioned into the first and second codon positions together (partition CP_{12}) and the third codon position (CP_3). For CP_{12} and CP_3, we used the nucleotide substitution models HKY + I (HKY, Hasegawa *et al.* 1985) and GTR + I + G (GTR, Tavaré 1986), respectively, selected based on the Akaike information criterion in JMODELTEST 2.1.3 (Posada 2008). The demography along the course of divergence was modelled by constant-sized populations between sequential splits, namely the piecewise-constant (PC) model. We used the extinction-free constant-rate birth process (Yule 1924) as a prior for divergence, and, under a strict clock model, we calibrated the root of the taxon tree with a lognormal prior of log (mean) = 0.96 and log (standard deviation) = 0.15, corresponding to an mtDNA-based estimate of the split time between *M. eleryi* and the common ancestor of *M. gracilis* and *M. recondita* as 2.62 (95% CI: 1.86–3.48) million years ago (Ma) (see Systematic notes on the focal species in Appendix S1, Supporting information). We performed two replicate MCMC runs in BEAST 1.7.4 (Drummond *et al.* 2012), each with 100 million iterations (8000 iterations per sample) and the first 10% of runs discarded as burn-in. We examined the runs in TRACER 1.5 (Rambaut & Drummond 2007) as well as with the 'starbeast_demog_log' python script in the biopy 0.1.7 package (available from: http://code.google.com/p/biopy/); these two runs gave consistent results and so were combined to give an effective sample size (ESS) of >2600 per parameter.

Nuclear markers for investigating divergence within the Murina gracilis complex

For insights into the divergence process in the nuclear genome among the focal taxa, we developed a set of 10 anonymous autosomal markers based on microsatellite flanking regions (A4, A9, A104, A109, A118, A122, B5, B114, B124 and D117). For each locus, we designed new primer pairs based on clone sequences to amplify the flanker but to exclude the microsatellite motif (Table S3, Supporting information). Primer pairs designed for A9 and A122 amplified fragments that overlap with those described in the earlier section.

For *M. gracilis* and *M. recondita*, we obtained sequences for each of the 10 loci by high-throughput 454-pyrosequencing (Margulies *et al.* 2005). Given that both species show strong geographic substructure within Taiwan (Kuo *et al.* 2014), which would violate assumptions of coalescent-based analyses, sequences were only generated for 15 individuals of each taxon from part of their respective ranges (Table 1). To sort sequences, we incorporated unique 3-bp tags at the 5′ end of the synthesized forward primer for each locus. For *M. gracilis*, we used the tags ACA, ACG, ACT, AGA, AGC, AGT, ATA, ATC, ATG, CGA, CGC, CGT, CTA, CTC and CTG, while for *M. recondita*, we used CAT, GTA, GTC, GTG, GAC, GAG, GAT, GCA, GCG, GCT, TAC, TAG, TAT, TCA and TCG. PCR products of each locus were visualized on a gel and pooled for 454-pyrosequencing at Mission Biotech (Taipei, Taiwan) on a 454 GS Junior System (Roche/454 Life Sciences).

We used the software CLC GENOMICS WORKBENCH 4.9 (CLC bio, Denmark) to filter and sort 454 reads as follows. First, we used original clone sequences as references on which 454 reads were mapped with a coverage parameter of 0.6 and a similarity parameter of

0.9. Second, we sorted mapped sequences into individual bats on the basis of the 3-bp tag plus 2–3 sites of the 5′ end of the forward primer. Sorted sequences were aligned using MUSCLE (Edgar 2004) in MEGA 5 (Tamura *et al.* 2011). For each individual, 50 reads were trimmed and aligned (in cases where fewer reads were available, <50 were used), and, assuming that error rates per nucleotide were lower than correct base calls (Galan *et al.* 2010), we inferred the haplotypes of every bat for each of its two chromosomes. We adopted the following conservative criteria for acceptance of haplotypes for downstream genetic analyses: (i) for each individual, only inferred haplotypes with frequencies of ≥5 were accepted such that the occurrence of two haplotypes ≥5 signified a heterozygote, and (ii) each individual was considered homozygous for a locus when only one haplotype was detected with a frequency of ≥10. Bats that did not meet these criteria, because only one haplotype was detected at a frequency of ≥5 but <10, were considered to be potentially heterozygous but with missing data for one of the two chromosomes.

We also sequenced the same 10 loci in *M. eleryi* using Sanger sequencing (Table 1) and confirmed in a subset of individuals of *M. gracilis* and *M. recondita* that both sequencing methods gave consistent results. PCR products were sequenced in both directions at Eurofins MWG Operon. In four of the 10 loci, indels (1–9 bp) were observed, with individuals heterozygous for such indels showing characteristic double peaks in downstream stretches on their chromatograms. In these individuals, we were able to deduce the nucleotide sequences of each haplotype based on the rationale that the superposed signatures would correspond to two nucleotides that differed by a length equal to that of the indel (Flot *et al.* 2006). Where two haplotypes could not be inferred in this way, we used PHASE (see earlier section), treating the two clades of *M. eleryi* that were identified and are hereafter referred to as *M. eleryi* 1 and 2 (see Results).

Final alignments of each of the 10 nuclear markers contained samples of *M. gracilis*, *M. recondita*, *M. eleryi* 1 and *M. eleryi* 2. Excluding indels, we assessed the genetic variability of each taxon at each locus based on the number of segregating sites, Watterson's (1975) theta value and nucleotide diversity, all calculated in DNASP 5.10.01 (Librado & Rozas 2009). We also used NETWORK to construct (ε = 10) locus-wise MJ genealogies for samples of all four taxa to gain information on genetic differences among them. Polzin & Daneshmand's (2003) maximum parsimony algorithm was used to remove unnecessary links in the network for one locus (A122) for which complex connections were seen.

Prior to subsequent coalescent-based analyses, for each locus, we tested for recombination using Hudson & Kaplan's (1985) four-gamete test assuming an infinite-site model of evolution, as implemented in the software IMGC (Woerner *et al.* 2007), in each case retaining the largest recombination-free block of sequences. This approach was not applied to locus A122, due to the detection of a tri-allelic segregating site that suggested this locus did not evolve in an infinite-site manner and might experience a faster mutation rate (also corroborated by analyses of genetic variability in the four focal taxa; see Results). Throughout this study, the HKY model was used for nucleotide substitutions for A122.

Divergence among taxa within the Murina gracilis complex revealed by ncDNA

The order of divergence among focal taxa was inferred in *BEAST, using the recombination-free sequences from 10 nuclear loci, and with a JC nucleotide substitution model (Jukes & Cantor 1969) applied to each except for A122. For demographic analysis throughout divergence, we used the PC model (see Selection of a demographic model for the ncDNA *BEAST analysis in Appendix S1, Supporting information for details of model selection). For calibration of multilocus coalescence events, we specified, for each locus, a strict clock with the clock rate sampled from the following lognormal prior: log (mean) = −6.12, log (standard deviation) = 0.58. This prior was set for a mean estimate of the neutral mutation rate of mammalian nuclear genomes as 0.0022 substitutions per site per million years (Kumar & Subramanian 2002) while allowing rates to vary among loci to an order of magnitude. Two replicate *BEAST runs were combined to give an ESS of >200 per parameter. Finally, a generation time for the focal taxa as 2 years was used to calculate the effective population sizes from the estimated demographic parameters.

Using the phylogeny estimated in *BEAST: ([(*M. recondita*, *M. eleryi* 1), *M. eleryi* 2], *M. gracilis*), we then inferred the divergence process among these taxa in further detail, and specifically to estimate gene flow among them, we used IM models implemented in IMa2-8.26.11 (Hey & Nielsen 2007; Hey 2010b). An infinite-site model was adopted for each of the 10 loci analysed except for A122. Truncated uniform priors for entry demographic parameters of IMa2 were set following the author's recommendations (Hey 2011); specifically, we set upper bounds of priors for the composite parameter of the split time (with the flag *−t*), the rescaled migration rate in either direction (*−m*), and the population mutation rate for each of the extant/ancestral taxa (*−q*) based on the genetic variability of *M. eleryi* 1, which had highest genetic variability of the four species (see Results). The geometric mean of Watterson's (1975) theta values over loci—an estimate for the

population mutation rate—was 0.0055 per nucleotide site, corresponding to a value of 1.1 per locus given a geometric mean of sequence lengths over the 10 loci as 196. We set $-t2$ and $-q5$ for two and five times of the above estimates, respectively, and for postsplit migrations we set $-m2$ for a moderately high upper bound for the 2NM value, as $2NM = q \times m/2 = 1.1$ under the set '*m*' value. In addition, we explored a different *m* prior, modelled by an exponential distribution with a mean value of 0.5 (with flags $-j8$ $-m0.5$), which circumvents truncation of the marginal estimate by an upper bound and is justified under the expectation of low migration between diverging taxa (Hey 2010b).

We also applied IM models, with identical prior settings to those described above, to pairwise data sets of the four focal taxa. Divergence times estimated independently for pairwise taxa could inform the splitting order (Hey 2010a) and thus corroborate the taxon phylogeny inferred by *BEAST. Metropolis-coupling MCMC (MC^3) for all above four- and two-taxon IM runs was conducted with a geometric heating scheme for 60 chains (heating parameters $-ha0.95$ $-hb0.8$), with 1 million iterations discarded as burn-in followed by 5 million iterations for sampling (100 iterations per sample). Three (for four-taxon analyses) or two (for two-taxon analyses) replicate runs were performed under each prior setting for assessment of convergence. Given that replicate runs appeared to converge, we combined results under each specific setting using the 'L mode' function of IMa2, and ran likelihood ratio tests (LRT) to assess evidence of postsplit gene flow between focal taxa, following Nielsen & Wakeley (2001). Finally, to convert entry demographic parameters into interpretable scales, we applied a mutation rate of 0.0022 per nucleotide site per million years (Kumar & Subramanian 2002), a geometric mean of sequence lengths of 196 bp and a generation time of 2 years.

Results

Assessment of contemporary gene flow between Murina gracilis and Murina recondita

Clustering analyses of 14 microsatellite loci yielded two different configurations at $K = 3$ and also at $K = 4$ (Fig. 1). In each of these cases, lower 'penalized log-likelihood values' (Pritchard *et al.* 2000) were obtained for a configuration with an empty cluster that contained no substantial fraction of any individual bat of either species. By excluding runs with empty clusters (Guillot 2008), the penalized log-likelihood was highest at $K = 4$ in which four *Murina recondita* individuals (labelled as RA, RB, RC and RD in Fig. 1) showed >10% of their genetic composition appearing to originate from *Murina gracilis*. All other bats of both species were assigned almost exclusively to genetic clusters of their own species (each with a sum of ancestry coefficients *q* for its own species >0.9).

Repeated STRUCTURE analyses with each locus sequentially removed revealed that apparent genetic admixture among some *M. gracilis* and *M. recondita* individuals was mainly attributable to loci A9 and A122 (Fig. 1; Table S4, Supporting information). To determine whether these signatures stemmed from introgression, we sequenced the flanking regions of A9 and A122 in selected bats (shown by arrows in Fig. 1) and constructed MJ networks. In the network based on A9, haplotypes of *M. gracilis* and *M. recondita* clustered by species; however, *M. recondita* showed an unexpected affiliation with *Murina eleryi* (Fig. 2). Similarly, for the A122 network, all *M. recondita* haplotypes clustered together with the exception of one that grouped with *M. eleryi* (Fig. 2). It follows that apparent signatures of genetic admixture between *M. gracilis* and *M. recondita* seen in multilocus microsatellite genotypes were not supported by analyses

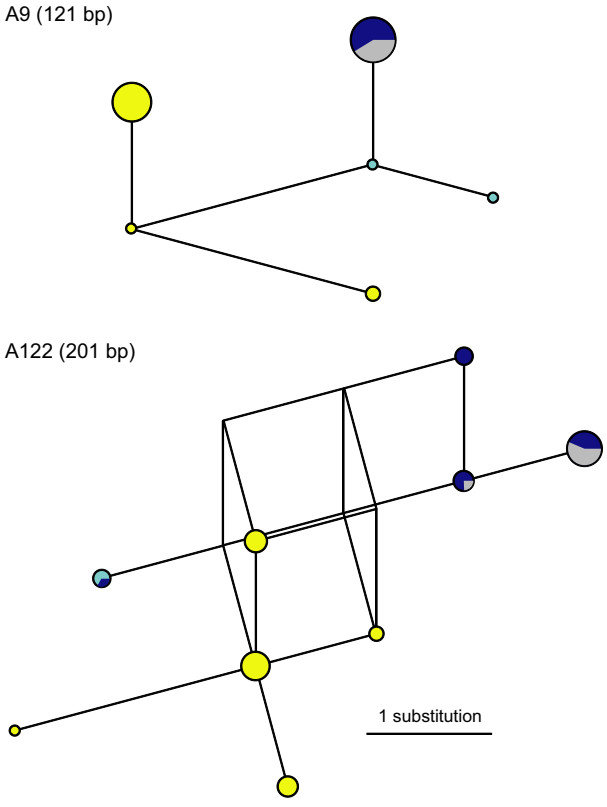

Fig. 2 Median-joining networks based on flanking regions of microsatellite loci A9 and A122. Circles are coloured to represent haplotypes of *Murina gracilis* (yellow), *Murina eleryi* (light blue), four individuals of *Murina recondita* labelled as RA, RB, RC and RD in Fig. 1 (grey) and remaining individuals of *M. recondita* (dark blue). Sizes of circles are proportional to sample sizes of unique haplotypes. The scale bar applies to both networks.

of these microsatellites' flanker sequences, suggesting they reflect microsatellite allele SH rather than true introgression. At the same time, however, we discovered an unexpectedly close relationship between *M. recondita* and *M. eleryi* that could be due to introgression. Based on this finding, we expanded sampling of *M. eleryi* in subsequent analyses to dissect the divergence history among all these *Murina* species.

Divergence within the Murina gracilis complex revealed by mtDNA

Using *BEAST, the concatenated mitochondrial sequences of Cyt-*b* and COI (Table 1) recovered a mtDNA genealogy (not shown) with four maximally supported monophyletic groups (posterior probability = 1) representing *M. gracilis*, *M. recondita* and *M. eleryi* from southern China (*M. eleryi* 1) and *M. eleryi* from Central Vietnam (*M. eleryi* 2). Among these lineages, *M. gracilis* and *M. recondita* grouped together with maximal support, as did the two *M. eleryi* lineages. These relationships were also recovered in the inferred species tree (posterior probabilities >0.99; see Fig. 3a). These two split events had median estimates of 0.79 (95% CI: 0.31–1.29) and 0.43 (95% CI: 0.10–0.77) Ma, respectively (Fig. 3a). Effective population sizes for extant and ancestral taxa ranged from 51 000 (*M. eleryi* 1) to 250 000 (*M. recondita*) as shown in Fig. 3a.

ncDNA structure within the Murina gracilis complex

454-pyrosequencing of autosomal microsatellite flanker sequences in larger sample sets of *M. gracilis* and *M. recondita* generated 73 395 reads, which were assembled to yield haplotypes for all 10 target loci from both chromosomes in all but one individual of *M. gracilis* and 75% of individuals of *M. recondita*. Sanger sequencing of orthologous sequences in *M. eleryi* yielded haplotypes from both chromosomes in 70% of individuals (see Table 1).

Locus-specific MJ networks supported pilot sequencing of two loci, confirming that *M. recondita* ncDNA sequences were typically more related to those of *M. eleryi* than to those of *M. gracilis* (Fig. S1, Supporting information). For three of 10 loci, *M. recondita* shared haplotypes with the two *M. eleryi* lineages but not with *M. gracilis*, and in cases where *M. recondita* shared haplotypes with *M. gracilis*, these haplotypes were also shared by the two *M. eleryi* lineages. At most loci, *M. eleryi* 1 and *M. eleryi* 2 had contrasting haplotype composition, indicative of divergence. Locus-wise measures of genetic variability for the four taxa are shown in Table 2. *Murina recondita* had a lower level of genetic variability than all the others, particularly reflected by its lower θ_S and π values at most of the 10 markers. Four-gamete tests suggested potential intralocus recombination at loci A4, A104, A109 and B124, for which relevant sections of alignments (for A4 and A109) or individual sequences (for A104 and B124) were removed using IMGC (shown in Fig. S1, Supporting information).

Divergence in Murina gracilis complex revealed by ncDNA

Supporting the haplotype networks, the species tree reconstructed using *BEAST recovered a monophyletic clade containing *M. recondita* and both *M. eleryi* taxa (posterior probability = 1), which was estimated to have diverged from *M. gracilis* around 2.06 (95% CI: 1.13–3.19) Ma (Fig. 3b). Within the (*M. recondita* + *M. eleryi*) clade, *M. recondita* formed a moderately well-supported clade with *M. eleryi* 1 (posterior probability = 0.79) to the exclusion of *M. eleryi* 2. The split between *M. eleryi* 2 and the common ancestor of *M. recondita* and *M. eleryi* 1 was dated to 0.66 (95% CI: 0.28–1.14) Ma, while divergence between the latter two taxa was dated to 0.42 (95% CI: 0.16–0.77) Ma. Effective population sizes of lineages under the PC model ranged from 59 000 (*M. recondita*) to 632 000 (common ancestor of *M. recondita* and the two *M. eleryi* taxa) (see Fig. 3b).

To aid descriptions, hereafter we use the abbreviations 4PM2 and 4PME0.5 for four-taxon IM analyses specifying a truncated uniform prior (upper bound = 2) and an exponential prior (mean = 0.5), respectively. For focal demographic parameters estimated with the 4PM2 prior, we show summary statistics in Fig. 4 and present marginal distributions in Fig. S2 (Supporting information). Summary statistics of these demographic parameters from both 4PM2 and 4PME0.5 analyses are also presented in Table S5 (Supporting information). The marginal distribution for the postsplit migration parameter, *m*, was more compressed towards zero with 4PME0.5 than with 4PM2 prior, leading to a smaller estimate from 4PME0.5 analysis (a trend also reflected in the population migration rate, 2NM; see Table S5, Supporting information); this was true for all *m* parameters along the course of divergence although such compressions in marginal distributions were less apparent for those with peaks at zero. For all other demographic parameters including times of split and effective population sizes, similar estimates were obtained regardless of the prior used (Table S5, Supporting information).

From both 4PM2 and 4PME0.5 analyses, modal estimates for times of split indicated divergence between *M. recondita* and *M. eleryi* 1 (T1), between the common ancestor of these two taxa and *M. eleryi* 2 (T2), and between the common ancestor of three taxa and *M. gra-*

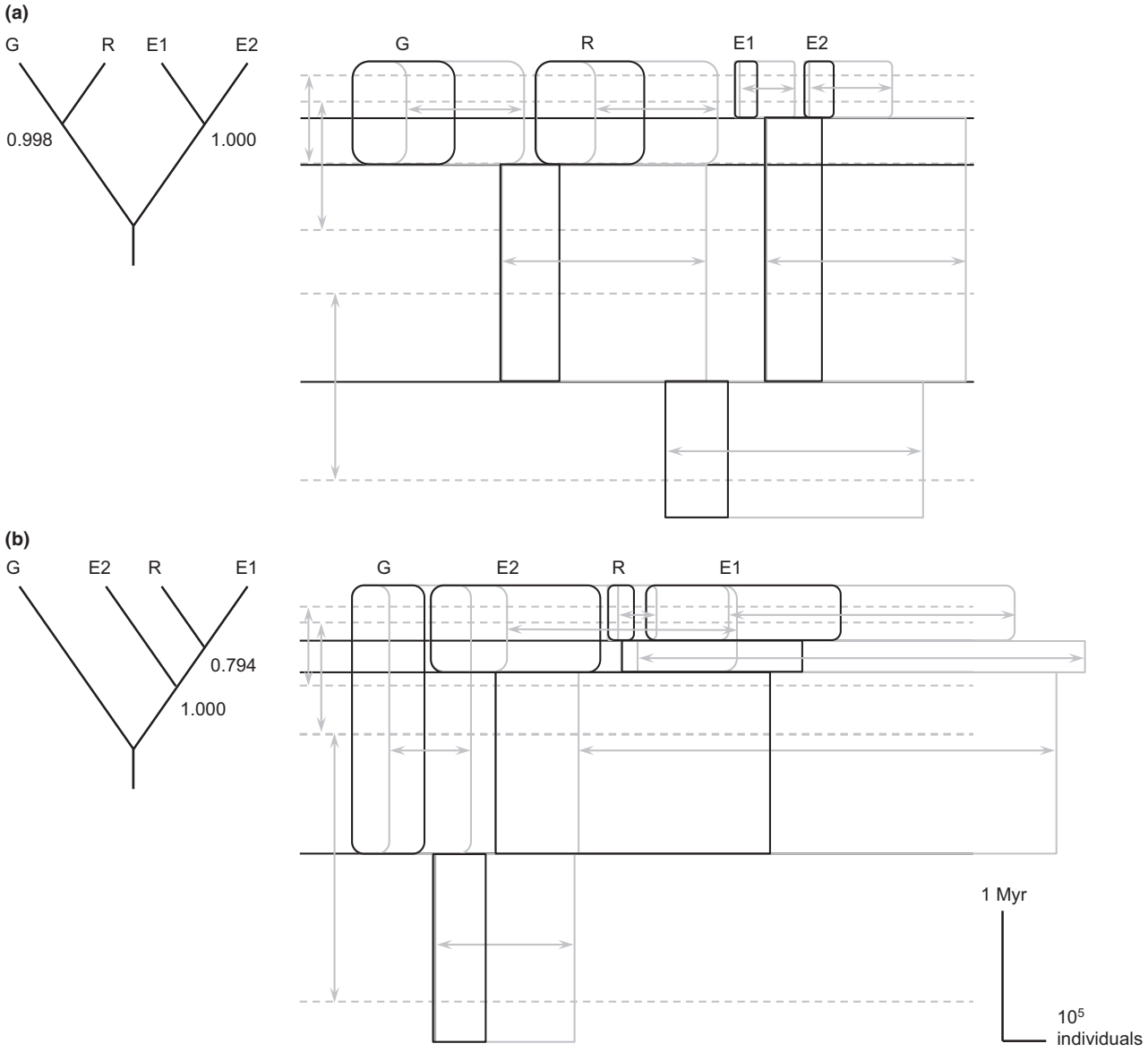

Fig. 3 Divergence within the *Murina gracilis* complex inferred from *BEAST analyses based on (a) mtDNA and (b) ncDNA. In each panel, extant taxa are labelled as G for *M. gracilis*, R for *Murina recondita*, E1 for *Murina eleryi* 1 and E2 for *M. eleryi* 2; the upper left corner shows the maximum clade credibility (MCC) topology with posteriors for specific taxon grouping, and the lower right corner shows demographic estimates obtained under corresponding MCC topology. In the demographic plots, horizontal and vertical dimensions are scaled to represent effective population sizes (boxes) and split times (horizontal lines; present time at the top), respectively. Black boxes and black horizontal lines are scaled to represent median estimates, while grey ones including lines with double arrows are scaled to present 95% confidence intervals of corresponding variables. Scale bars for 100 000 individuals and for 1 million years apply to both panels.

cilis (T3), at 1.2–1.4, 1.8–1.9, and around 2.3 Ma, respectively. Nevertheless, confidence sets for these parameters were rather broad (see Fig. 4 for values from 4PM2 analysis); this was especially true for T1 and T3 for which flat marginal distributions were obtained (see Fig. S2a, Supporting information for curves from 4PM2 analysis). Among a total of 18 *m* parameters, seven had nonzero modes under 4PM2: bidirectional migration between *M. recondita* and *M. eleryi* 1 and migration from *M. recondita* to *M. eleryi* 2, from *M. eleryi* 2 to *M. eleryi* 1, from *M. eleryi* 2 to the common ancestor of *M. recondita* and *M. eleryi* 1, from the common ancestor of *M. recondita* and *M. eleryi* 1 to *M. gracilis* and from the common ancestor of *M. recondita* and both *M. eleryi* taxa to *M. gracilis* (Fig. S2b, Supporting information). Of these seven, only the former four also had nonzero

Table 2 Genetic variability of four taxa in the *Murina gracilis* complex based on 10 microsatellite flanking regions. Values are calculated for each alignment showing no signature of intralocus recombination except for the locus A122. Estimates of θ_S and π are presented as corresponding raw values multiplied by 100

		M. gracilis				*Murina recondita*				*Murina eleryi* 1				*M. eleryi* 2			
Locus	*L*	*N*seq	*S*	θ_S	π	*N*seq	*S*	θ_S	π	*N*seq	*S*	θ_S	π	*N*seq	*S*	θ_S	π
A4	216	30	4	0.47	0.48	27	2	0.24	0.22	14	2	0.29	0.19	10	7	1.15	1.12
A9	102	29	3	0.75	1.22	15	0	0	0	14	3	0.93	0.97	10	2	0.69	0.55
A104	156	30	3	0.49	0.93	25	0	0	0	9	4	0.94	0.68	10	1	0.23	0.13
A109	137	30	2	0.37	0.45	30	1	0.18	0.05	14	3	0.69	0.40	6	2	0.64	0.49
A118	180	30	4	0.56	0.59	21	1	0.15	0.24	12	4	0.74	0.37	8	4	0.86	1.03
A122	184	30	5	0.69	0.63	24	7	1.02	0.86	6	10	2.38	2.86	10	7	1.35	1.88
B5	286	30	0	0	0	24	0	0	0	12	1	0.12	0.06	10	1	0.12	0.17
B114	318	30	0	0	0	23	1	0.09	0.16	12	2	0.21	0.27	8	4	0.49	0.60
B124	249	30	0	0	0	20	0	0	0	13	4	0.52	0.45	10	2	0.28	0.27
D117	234	30	4	0.43	0.42	29	0	0	0	12	5	0.71	0.86	8	5	0.82	0.93

L, sequence length in number of base pairs; *N*seq, sample sizes of sequences; *S*, number of segregating sites; θ_S, Watterson's (1975) theta; π, nucleotide diversity.

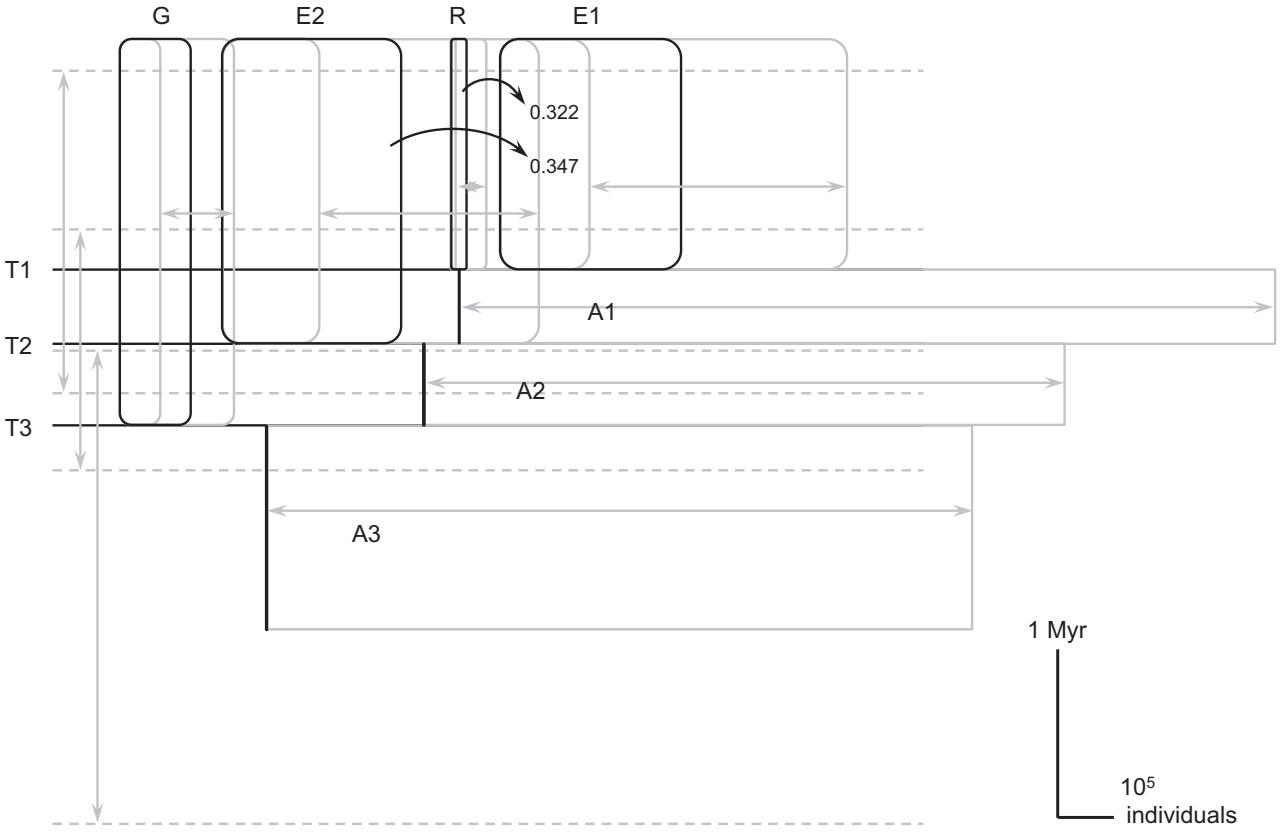

Fig. 4 Divergence within the *Murina gracilis* complex inferred from four-taxon isolation-with-migration (IM) analyses under the 4PM2 prior. Extant taxa are labelled as in Fig. 3 while ancestral populations are labelled as A1 for *Murina recondita* plus *Murina eleryi* 1, A2 for *M. recondita* plus both *M. eleryi* taxa, and A3 for all extant taxa. Split times are numbered to present successive divergence events from recent to ancient ones under the specified phylogeny—([(R, E1), E2], G). Horizontal and vertical dimensions are scaled as in Fig. 3 except that black boxes and black horizontal lines are scaled to present modal estimates. Black curved arrows mark directions of postsplit migrations, each of which was significant using the population migration rate (2NM) based on Nielsen & Wakeley's (2001) likelihood ratio test; modal estimates of these 2NM values are also given.

modes under 4PME0.5. Based on either *m* or 2NM, LRTs were significant for migrations from *M. recondita* to *M. eleryi* 1 and from *M. eleryi* 2 to *M. eleryi* 1 under both priors except for migration from *M. recondita* to *M. eleryi* 1 based on *m* under 4PME0.5. Nonsignificant results were obtained for all other LRTs (see Table S5, Supporting information for a summary of LRTs based on 2NM). Under the two priors used, effective population sizes for the extant taxa had modal estimates ranged from 27 000/33 000 (*M. recondita*) to 322 000/348 000 (*M. eleryi* 1) or 319 000/349 000 (*M. eleryi* 2) (Fig. 4; Table S5, Supporting information). For effective population sizes of ancestral populations, flat marginal distributions (Fig. S2c, Supporting information), and thus broad confidence intervals (Table S5, Supporting information), were obtained, suggesting little information from the data on these parameters.

As in the four-taxon IM analyses, we used the abbreviations 2PM2 and 2PME0.5 for two-taxon IM analyses specifying a truncated uniform prior (upper bound = 2) and an exponential prior (mean = 0.5), respectively. Summary statistics for all six pairs of taxa analysed under 2PM2 prior are shown in Fig. 5 while their marginal distributions are presented in Fig. S3 (Supporting information). A full list of summary statistics for all two-taxon analyses under the two priors used is given in Table S6 (Supporting information). Again, the marginal distribution for each *m* parameter was more compressed towards zero under 2PME0.5 than under 2PM2 prior, leaving smaller *m* estimates in the former analysis (see Table S6, Supporting information). For parameters of split times and effective population sizes, on the other hand, IM estimates were insensitive to the prior used (Table S6, Supporting information).

From two-taxon IM analyses, comparing modal estimates across data sets suggested that the order of splits among taxa was consistent with the results from ncDNA-based *BEAST; thus, *M. recondita* and *M. eleryi* 1 split most recently (1.1–1.2 Ma), then *M. eleryi* 2 and either *M. recondita* or *M. eleryi* 1 (1.4–1.5 Ma), and finally the most ancient split was between *M. gracilis* and either of the two *M. eleryi* lineages (1.5–1.7 Ma) (see Fig. 5 for values from 2PM2 analyses). Inconsistent with this inferred splitting order, modal estimates from two-taxon IM analyses suggested an unexpected recent divergence between *M. gracilis* and *M. recondita* (1.2–1.3 Ma). However, under either of the two priors used, the marginal distribution for the split time of *M. gracilis* and *M. recondita* was the flattest one among the six pairwise analyses (see Fig. S3a, Supporting information for curves from 2PM2 analyses), implying greater uncertainty underlying this estimate. When *M. gracilis* was paired with either of the other taxa, modal estimates of *m* were zero for both directions. In contrast, modal estimates of *m* for the remaining pairwise combinations of taxa were nonzero for both directions (Fig. S3b, Supporting information). Based on either *m* or 2NM, LRTs were significant for bidirectional migrations between

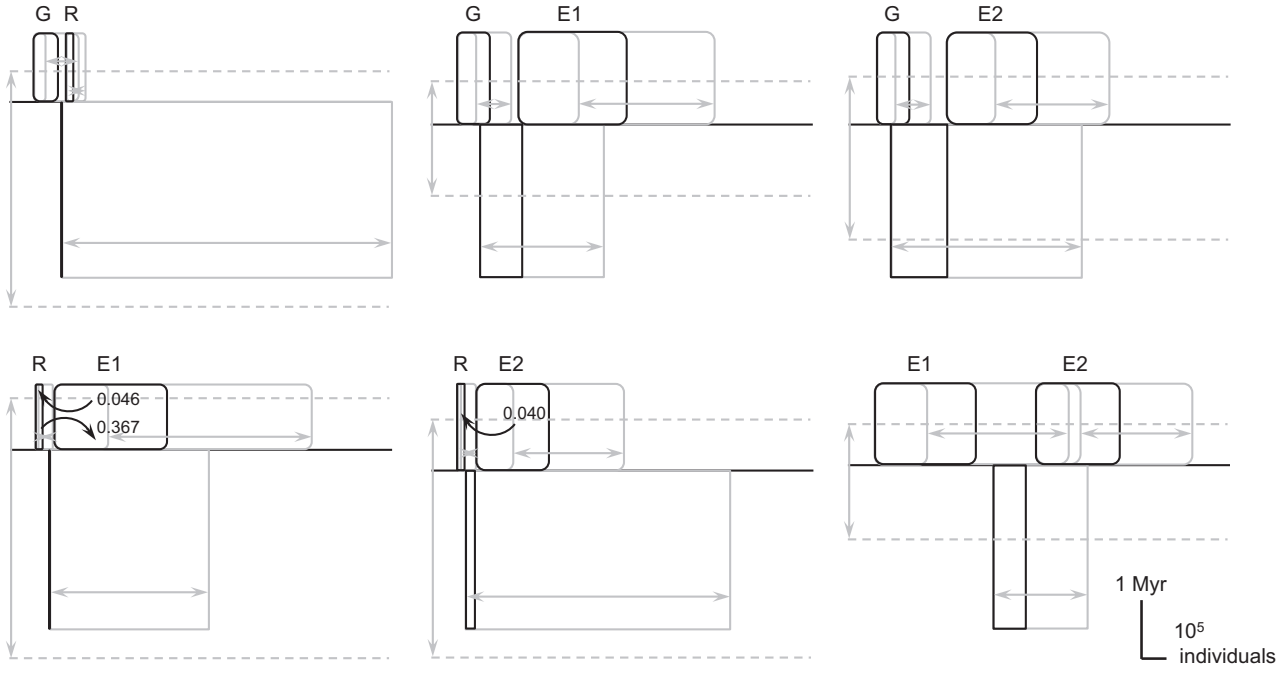

Fig. 5 Divergence within the *Murina gracilis* complex recovered by pairwise two-taxon isolation-with-migration (IM) analyses under the 2PM2 prior. For an explanation of the labels used and format of the plots, see Fig. 4. Scale bars for 100 000 individuals and for 1 million years apply to all six plots.

M. recondita and *M. eleryi* 1 and migration from *M. eleryi* 2 to *M. recondita* under both priors except for migration from *M. recondita* to *M. eleryi* 1 based on *m* under 2PME0.5. LRTs were also significant for bidirectional migrations between *M. eleryi* 1 and *M. eleryi* 2 based on 2NM under 2PME0.5 (Table S6, Supporting information). Two-taxon IM analyses gave effective population size estimates for *M. gracilis*, *M. recondita* and *M. eleryi* 2 broadly consistent with those from four-taxon analyses. In contrast, the estimates for *M. eleryi* 1 were higher than obtained from four-taxon analyses (Table S6, Supporting information). As with the four-taxon models, two-taxon analyses gave diffuse marginal distributions for effective population sizes of ancestral populations (Fig. S3c, Supporting information), suggesting limited information about these parameters was available from the data.

Discussion

Cases of geographical confinement of sister taxa to islands are rare and have been proposed as candidate systems in which nonallopatric speciation processes could have occurred (White 1978; Coyne & Price 2000; Coyne 2007). Here, we examined the process of divergence between the tube-nosed bats *Murina gracilis* and *Murina recondita*, both of which are endemic to Taiwan and which, based on phylogenetic reconstructions of mtDNA, appear to be sister species (Kuo 2004, 2013). To determine whether these taxa did indeed form in the face of migration, consistent with nonallopatric speciation, we tested for gene flow at different temporal scales using a variety of molecular markers and statistical approaches. Tests for contemporary gene flow based on ncDNA uncovered an unexpected sister relationship between *M. recondita* and a continental species *Murina eleryi*, to the exclusion of *M. gracilis*. The demographic process and putative mechanisms responsible for this mtDNA-ncDNA conflict are discussed below.

Absence of recent introgressive hybridization between Murina gracilis and Murina recondita

Although, for the most part, microsatellite-based clustering suggested little, if any, contemporary gene flow between *M. gracilis* and *M. recondita* (250 individual bats in total; Fig. 1), a small number of individuals of *M. recondita* did appear to show mixed ancestry with *M. gracilis* (Fig. 1 and Table S4, Supporting information). Such cases of apparent genetic admixture based on microsatellite clustering are not unusual and are typically attributed to introgression or the retention of ancestral polymorphism (e.g. Muir & Schlötterer 2005; Berthier *et al.* 2006; Randi 2008; Brown *et al.* 2010; Bogdanowicz *et al.* 2012). In our study, however, sequencing and analyses of the respective *M. recondita* microsatellite flanking regions—which are expected to evolve more slowly than their adjacent microsatellite motifs (Estoup *et al.* 2002)—did not support admixture. Instead, in networks based on these flanking regions, the two putative sister taxa were reciprocally monophyletic with respect to each other (Fig. 2). It follows that apparent admixture signatures based on microsatellite genotyping appear to stem from allele size homoplasies, a well-described phenomenon that is nonetheless infrequently tested for and described in studies of population structure (exceptions include Adams *et al.* 2004; Rossiter *et al.* 2007).

Divergence between Murina gracilis and Murina recondita

Further clustering analyses of 10 microsatellite flanking sequences, in which both focal taxa were included along with the mainland congener *M. eleryi*, recovered an unexpected grouping of the latter with *M. recondita*. Specifically, phylogenetic reconstruction performed in *BEAST—an approach that simultaneously reconstructs the gene tree(s) and evaluates the support of different species trees in generating such a gene tree (or gene trees) through stochastic drift (Heled & Drummond 2010; Drummond *et al.* 2012)—indicated that *M. recondita* formed a monophyletic clade with *M. eleryi* 1 from southern mainland China, which in turn formed a clade with *M. eleryi* 2 from Central Vietnam to the exclusion of *M. gracilis* (Fig. 3b). Additional supporting evidence for this history of divergence came from ncDNA-based two-taxon IM analyses (Figs 5 and S3a, Supporting information) by which split times of divergent taxa were estimated while accounting for the potential influences of postsplit gene flow (Hey & Nielsen 2004, 2007). It is important to recognize that these estimated split times had broad confidence intervals, indicative that the data contains limited information about these parameters. Further uncertainty in these estimates arises from the fact that they were solely informed by a mean multilocus mutation rate. Despite uncertainty about these split times, however, it is noteworthy that the IM and *BEAST analyses of microsatellite flanking sequences both suggested the same order of divergence; thus, the mitochondrial and nuclear genomes harboured conflicting signals about the divergence process of the focal taxa.

By superimposing the mtDNA genealogy for the four focal taxa on the splitting order obtained by the ncDNA, we were able to infer a scenario of independent incursions of the Taiwanese species. *Murina gracilis* appears to have colonized first, followed by *M. recondita* with massive mtDNA introgression from the former to

the latter. The clustering of range-wide mtDNA haplotypes of both Taiwanese species to the exclusion of those from *M. eleryi* implies that the mitochondrial genomes of *M. recondita* have been completely replaced by those of *M. gracilis*. Meanwhile, the present reciprocally monophyletic relationship between the two Taiwanese species indicates that any introgression has since ceased, probably around 0.3–1.3 (median: 0.8) Ma (Fig. 3a: split between *M. gracilis* and *M. recondita*). In contrast, neither the two-taxon nor four-taxon IM analyses detected postsplit nuclear gene flow between *M. gracilis* and *M. recondita* (Figs 4 and 5, respectively).

Like all species of their genus, *M. gracilis* and *M. recondita* show a suite of ecomorphological adaptations for living in the forest interior, including broad wings and very large call bandwidths for detecting arthropods in dense clutter (Kingston *et al.* 1999, 2003; Schmieder *et al.* 2010). At the same time, however, such traits are associated with reduced gene flow (Struebig *et al.* 2011) and are likely to constrain the ability of these bats to move across more open environments, including water bodies such as the Taiwan Strait. It follows that the two inferred incursions will almost certainly have occurred during glacial periods when the drop in sea level exposed the continental shelf connecting Taiwan and mainland Asia (Voris 2000). Consequently, rather than diverging nonallopatrically on Taiwan, as we initially hypothesized based on their restricted island distributions, *M. gracilis* and *M. recondita* appear to have speciated during a period of geographical isolation, with their codistribution arising via secondary contact. Similar histories of double incursions for pairs of congeneric Taiwanese taxa have been inferred in rodents (genera *Apodemus* and *Niviventer*; Yu 1995) and grass lizards (genus *Takydromus*; Lue & Lin 2008), both of which showed a paraphyletic relationships among island taxa with respect to continental forms.

Several scenarios may account for the observed massive introgression of mtDNA, yet little or no introgression of ncDNA, from *M. gracilis* to *M. recondita*. First, mitochondrial replacement can arise due to positive selection (e.g. reviewed in Melo-Ferreira *et al.* 2014). Despite finding no evidence of positive selection at mtDNA, we cannot rule this out (Tests of positive selection in Appendix S1, Supporting information), especially given that mitochondrial protein-coding genes are subject to genetic hitch-hiking due to a lack of recombination that characterizes mitogenomes (Galtier *et al.* 2009). Alternatively, contrasting levels of mtDNA and ncDNA introgression can also reflect asymmetries between species in the extent to which they undergo assortative mating, or experience sex-biased reductions in hybrid fitness (Chan & Levin 2005; Mallet 2005). Perhaps the simplest explanation for the observed discordance between mtDNA and ncDNA markers lies in the fact that the two Taiwanese species would have experienced different demographic conditions when they colonized Taiwan, as expected given the inferred scenario of two temporally distinct incursions. Specifically, it is probable that during the incursion of Taiwan by *M. recondita*, this colonizing taxon will have been in a phase of relative demographic growth compared to the earlier arriving *M. gracilis*. Simulations by Currat *et al.* (2008) show that under such conditions, introgression occurs from resident to the colonizing population. While massive mtDNA introgression from *M. gracilis* to *M. recondita* could have occurred via such 'allele surfing', a lack of parallel ncDNA introgression could be attributed to male-biased gene flow among conspecific populations of the latter species (Tests for sex-biased dispersal in *M. gracilis* and *M. recondita* in Appendix S1, Supporting information), so that *M. gracilis* nuclear alleles introgressed would have faced competition from those sent from *M. recondita* populations and thus reduced their chance of fixation. Indeed, evidence for the influence of sex-biased dispersal on differential rates of introgression among markers with different modes of inheritance has been reported in a wide range of taxa (Petit & Excoffier 2009). Further studies are needed to disentangle the contributions of these potential mechanisms between *M. gracilis* and *M. recondita*.

Introgression in tube-nosed bats and other bat species

Introgression was not only inferred for *M. gracilis* to *M. recondita*. Our four-taxon IM analyses also suggested postsplit nuclear gene flow from *M. recondita* to the continental *M. eleryi*, as well as between divergent clades of *M. eleryi* (Fig. 4). We therefore speculate that levels of mtDNA introgression might be even higher in these cases, based again on insights and expectations from simulations (Currat *et al.* 2008). In the former of these cases, more sampling of *M. eleryi* populations close to Taiwan is needed to test for mtDNA introgression. In the latter case, on the other hand, complete mitochondrial replacement between the two *M. eleryi* clades is implied by the observation that the estimated split times based on both two- and four-taxon models were substantially earlier than those estimated from mitochondrial genes. Unlike the situation between *M. gracilis* and *M. recondita* where mitochondrial replacement occurred over only tens of kilometres, any replacement between groups of *M. eleryi* would have involved much larger geographic distances of up to 900 km. Given that levels of introgression into invading species are known to fall with distance from the front wave of hybridization (Currat *et al.* 2008), it is likely that mitochondrial introgression in our focal bats is very efficient and prob-

ably facilitated by very low mtDNA gene flow among local populations (demonstrated in Kuo *et al.* 2014 for the two Taiwanese species).

Our study of *Murina* sister taxa adds to the mounting evidence for introgression in bats. Moreover, the inferred patterns—namely unidirectional rampant mtDNA introgression with little or no nuclear introgression—show similarities to those reported for species of the genera *Myotis* (Berthier *et al.* 2006) and *Rhinolophus* (Mao *et al.* 2013) as well as members of the family Pteropodidae (Nesi *et al.* 2011). Higher introgression of mtDNA than of ncDNA has also been implicitly suggested in other bat species (Larsen *et al.* 2010; Vallo *et al.* 2013), whereas higher levels of introgression at ncDNA than at mtDNA in bats appears to be much rarer (but see Hulva *et al.* 2010; Mao *et al.* 2010). Like in the case of *Murina*, Berthier *et al.* (2006) attributed elevated mtDNA introgression in *Myotis* to contrasting demographic dynamics between the invading vs. resident species, together with male-based gene flow among populations of the former taxon. However, it is important to recognize that multiple alternative scenarios might account for such patterns, leading Toews & Brelsford (2012) to call for a shift away from documenting further mitonuclear discordance towards hypothesis testing to rule out some explanations of common patterns.

Conclusions

Our analyses of gene flow at different temporal and spatial scales indicate that rather than diverging on Taiwan, the two endemic and closely related *Murina* species are a product of vicariant speciation from a period of isolation. Consequently, the current range overlap stems from multiple incursions, while the previously accepted sister relationship based on mtDNA is incorrect and was obscured by mitochondrial introgression coupled with a lack of wider sampling of geographically distant continental taxa. This example reveals how historical processes of vicariance, colonization and hybridization can readily lead to misleading signatures of nonallopatric speciation, thus highlighting the need for careful analyses to distinguish among such scenarios. Further caution comes from simulations of bird range data showing that even true sister taxa that have speciated in allopatry can readily show partial range overlap and, occasionally, complete range overlap (Phillimore *et al.* 2008). It is perhaps unsurprising, therefore, that many of the most plausible cases of divergence with gene flow come from plants attributed to their greater tendency for fine-scale niche divergence (Anacker & Strauss 2014). Nonetheless, even in the most convincing and well-studied such examples, it is still not trivial to rule out the alternative explanation of double colonizations, particularly where introgression, extinction and/or incomplete sampling are also possibilities (see Papadopulos *et al.* 2011).

Acknowledgements

We thank Ian Barnes, Michael Bruford, Kalina Davies and Richard Nichols for helpful comments on this work. HCK was supported by the Overseas Research Students Awards Scheme and the University of London Central Research Fund as well as by the Studying Abroad Scholarship from the Taiwanese Ministry of Education. GC received support from the SYNTHESYS Project, which is financed by the European Community Research Infrastructure Action under the FP7 'Capacities' Program, and from the Hungarian Scientific Research Fund (OTKA) K112440. This research was also funded by a grant to SFC, YPF and SJR from the Taiwanese Ministry of Science and Technology (NSC 100-2621-B-126-001).

References

Adams RI, Brown KM, Hamilton MB (2004) The impact of microsatellite electromorph size homoplasy on multilocus population structure estimates in a tropical tree (*Corythophora alta*) and an anadromous fish (*Morone saxatilis*). *Molecular Ecology*, **13**, 2579–2588.

Anacker BL, Strauss SY (2014) The geography and ecology of plant speciation: range overlap and niche divergence in sister species. *Proceedings of the Royal Society of London B: Biological Sciences*, **281**, 20132980.

Barraclough TG, Vogler AP (2000) Detecting the geographical pattern of speciation from species-level phylogenies. *The American Naturalist*, **155**, 419–434.

Berthier P, Excoffier L, Ruedi M (2006) Recurrent replacement of mtDNA and cryptic hybridization between two sibling bat species *Myotis myotis* and *Myotis blythii*. *Proceedings of the Royal Society B-Biological Sciences*, **273**, 3101–3109.

Bogdanowicz W, Piksa K, Tereba A (2012) Hybridization hotspots at bat swarming sites. *PLoS ONE*, **7**, e53334.

Brown RM, Nichols RA, Faulkes CG *et al.* (2010) Range expansion and hybridization in Round Island petrels (*Pterodroma* spp.): evidence from microsatellite genotypes. *Molecular Ecology*, **19**, 3157–3170.

Chan KMA, Levin SA (2005) Leaky prezygotic isolation and porous genomes: rapid introgression of maternally inherited DNA. *Evolution*, **59**, 720–729.

Coyne JA (2007) Sympatric speciation. *Current Biology*, **17**, R787–R788.

Coyne JA, Price TD (2000) Little evidence for sympatric speciation in island birds. *Evolution*, **54**, 2166–2171.

Currat M, Ruedi M, Petit RJ, Excoffier L (2008) The hidden side of invasions: massive introgression by local genes. *Evolution*, **62**, 1908–1920.

Dieckmann U, Doebeli M (1999) On the origin of species by sympatric speciation. *Nature*, **400**, 354–357.

Drummond AJ, Suchard MA, Xie D, Rambaut A (2012) Bayesian phylogenetics with BEAUti and the BEAST 1.7. *Molecular Biology and Evolution*, **29**, 1969–1973.

Edgar RC (2004) MUSCLE: multiple sequence alignment with high accuracy and high throughput. *Nucleic Acids Research*, **32**, 1792–1797.

Eger JL, Lim BK (2011) Three new species of *Murina* from southern China (Chiroptera: Vespertilionidae). *Acta Chiropterologica*, **13**, 227–243.

Estoup A, Jarne P, Cornuet JM (2002) Homoplasy and mutation model at microsatellite loci and their consequences for population genetics analysis. *Molecular Ecology*, **11**, 1591–1604.

Fitzpatrick BM, Fordyce JA, Gavrilets S (2009) Pattern, process and geographic modes of speciation. *Journal of Evolutionary Biology*, **22**, 2342–2347.

Flot J-F, Tillier A, Samadi S, Tillier S (2006) Phase determination from direct sequencing of length-variable DNA regions. *Molecular Ecology Notes*, **6**, 627–630.

Fluxus Technology Ltd. (2010) *Network*. Available from http://www.fluxus-engineering.com/sharenet.htm.

Forbes AA, Powell THQ, Stelinski LL, Smith JJ, Feder JL (2009) Sequential sympatric speciation across trophic levels. *Science*, **323**, 776–779.

Francis CM, Borisenko AV, Ivanova NV *et al.* (2010) The role of DNA barcodes in understanding and conservation of mammal diversity in Southeast Asia. *PLoS ONE*, **5**, e12575.

Furey NM, Thong VD, Bates PJJ, Csorba G (2009) Description of a new species belonging to the *Murina* 'suilla-group' (Chiroptera: Vespertilionidae: Murininae) from North Vietnam. *Acta Chiropterologica*, **11**, 225–236.

Galan M, Guivier E, Caraux G, Charbonnel N, Cosson J-F (2010) A 454 multiplex sequencing method for rapid and reliable genotyping of highly polymorphic genes in large-scale studies. *BMC Genomics*, **11**, 296.

Galtier N, Nabholz B, Glemin S, Hurst GDD (2009) Mitochondrial DNA as a marker of molecular diversity: a reappraisal. *Molecular Ecology*, **18**, 4541–4550.

Garrick RC, Sunnucks P, Dyer RJ (2010) Nuclear gene phylogeography using PHASE: dealing with unresolved genotypes, lost alleles, and systematic bias in parameter estimation. *BMC Evolutionary Biology*, **10**, 118.

Gavrilets S, Waxman D (2002) Sympatric speciation by sexual conflict. *Proceedings of the National Academy of Sciences of the USA*, **99**, 10533–10538.

Geraldes A, Ferrand N, Nachman MW (2006) Contrasting patterns of introgression at X-linked loci across the hybrid zone between subspecies of the European rabbit (*Oryctolagus cuniculus*). *Genetics*, **173**, 919–933.

Guillot G (2008) Inference of structure in subdivided populations at low levels of genetic differentiation-the correlated allele frequencies model revisited. *Bioinformatics*, **24**, 2222–2228.

Hasegawa M, Kishino H, Yano TA (1985) Dating of the human-ape splitting by a molecular clock of mitochondrial DNA. *Journal of Molecular Evolution*, **22**, 160–174.

Heled J, Drummond AJ (2010) Bayesian inference of species trees from multilocus data. *Molecular Biology and Evolution*, **27**, 570–580.

Hey J (2006) Recent advances in assessing gene flow between diverging populations and species. *Current Opinion in Genetics & Development*, **16**, 592–596.

Hey J (2010a) The divergence of chimpanzee species and subspecies as revealed in multipopulation isolation-with-migration analyses. *Molecular Biology and Evolution*, **27**, 921–933.

Hey J (2010b) Isolation with migration models for more than two populations. *Molecular Biology and Evolution*, **27**, 905–920.

Hey J (2011) *Documentation for IMa2*. Available from https://bio.cst.temple.edu/~hey/program_files/IMa2/Using_IMa2_8_24_2011.pdf.

Hey J, Nielsen R (2004) Multilocus methods for estimating population sizes, migration rates and divergence time, with applications to the divergence of *Drosophila pseudoobscura* and *D. persimilis*. *Genetics*, **167**, 747–760.

Hey J, Nielsen R (2007) Integration within the Felsenstein equation for improved Markov chain Monte Carlo methods in population genetics. *Proceedings of the National Academy of Sciences of the USA*, **104**, 2785–2790.

Hudson RR, Kaplan NL (1985) Statistical properties of the number of recombination events in the history of a sample of DNA sequences. *Genetics*, **111**, 147–164.

Hulva P, Fornuskova A, Chudarkova A *et al.* (2010) Mechanisms of radiation in a bat group from the genus *Pipistrellus* inferred by phylogeography, demography and population genetics. *Molecular Ecology*, **19**, 5417–5431.

Husband BC, Sabara HA (2004) Reproductive isolation between autotetraploids and their diploid progenitors in fireweed, *Chamerion angustifolium* (Onagraceae). *New Phytologist*, **161**, 703–713.

Jackson DE (2008) Sympatric speciation: perfume preferences of orchid bee lineages. *Current Biology*, **18**, R1092–R1093.

Jakobsson M, Rosenberg NA (2007) CLUMPP: a cluster matching and permutation program for dealing with label switching and multimodality in analysis of population structure. *Bioinformatics*, **23**, 1801–1806.

Jukes TH, Cantor CR (1969) Evolution of protein molecules. In: *Mammalian Protein Metabolism* (ed. Munro HH), pp. 21–132. Academic Press, New York, New York.

Kingston T, Rossiter SJ (2004) Harmonic-hopping in Wallacea's bats. *Nature*, **429**, 654–657.

Kingston T, Jones G, Akbar Z, Kunz TH (1999) Echolocation signal design in Kerivoulinae and Murininae (Chiroptera: Vespertilionidae) from Malaysia. *Journal of Zoology*, **249**, 359–374.

Kingston T, Francis CM, Akbar Z, Kunz TH (2003) Species richness in an insectivorous bat assemblage from Malaysia. *Journal of Tropical Ecology*, **19**, 67–79.

Kisel Y, Barraclough TG (2010) Speciation has a spatial scale that depends on levels of gene flow. *The American Naturalist*, **175**, 316–334.

Kumar S, Subramanian S (2002) Mutation rates in mammalian genomes. *Proceedings of the National Academy of Sciences of the USA*, **99**, 803–808.

Kuo H-C (2004) *Systematics of bats of genus Murina in Taiwan (Chiroptera: Vespertilionidae)*. MS Thesis, National Taiwan University, Taipei.

Kuo H-C (2013) *Phylogeography and diversification of Taiwanese bats*. PhD Thesis, Queen Mary, University of London, London.

Kuo H-C, Fang Y-P, Csorba G, Lee L-L (2009) Three new species of *Murina* (Chiroptera: Vespertilionidae) from Taiwan. *Journal of Mammalogy*, **90**, 980–991.

Kuo H-C, Chen S-F, Rossiter SJ (2013) Development and characterisation of microsatellite loci for *Murina gracilis* (Vespertilionidae) and cross-species amplification in two other

congeneric species. *Conservation Genetics Resources*, **5**, 1117–1120.

Kuo H-C, Chen S-F, Fang Y-P, Flanders J, Rossiter SJ (2014) Comparative rangewide phylogeography of four endemic Taiwanese bat species. *Molecular Ecology*, **23**, 3566–3586.

Larsen PA, Marchán-Rivadeneira MR, Baker RJ (2010) Natural hybridization generates mammalian lineage with species characteristics. *Proceedings of the National Academy of Sciences of the USA*, **107**, 11447–11452.

Librado P, Rozas J (2009) DnaSP v5: a software for comprehensive analysis of DNA polymorphism data. *Bioinformatics*, **25**, 1451–1452.

Llopart A, Elwyn S, Lachaise D, Coyne JA (2002) Genetics of a difference in pigmentation between *Drosophila yakuba* and *Drosophila santomea*. *Evolution*, **56**, 2262–2277.

Losos JB, Glor RE (2003) Phylogenetic comparative methods and the geography of speciation. *Trends in Ecology & Evolution*, **18**, 220–227.

Lue K-Y, Lin S-M (2008) Two new cryptic species of *Takydromus* (Squamata: Lacertidae) from Taiwan. *Herpetologica*, **64**, 379–395.

Lynch JD (1989) The gauge of speciation: on the frequencies of modes of speciation. In: *Speciation and Its Consequences* (eds Otte D, Endler JA), pp. 527–553. Sinauer Associates, Sunderland, Massachusetts.

Mallet J (2005) Hybridization as an invasion of the genome. *Trends in Ecology & Evolution*, **20**, 229–237.

Mao X, Zhang J, Zhang S, Rossiter SJ (2010) Historical male-mediated introgression in horseshoe bats revealed by multilocus DNA sequence data. *Molecular Ecology*, **19**, 1352–1366.

Mao X, He G, Zhang J, Rossiter SJ, Zhang S (2013) Lineage divergence and historical gene flow in the Chinese horseshoe bat (*Rhinolophus sinicus*). *PLoS ONE*, **8**, e56786.

Margulies M, Egholm M, Altman WE *et al.* (2005) Genome sequencing in microfabricated high-density picolitre reactors. *Nature*, **437**, 376–380.

Mattern MY, McLennan DA (2000) Phylogeny and speciation of felids. *Cladistics*, **16**, 232–253.

Melo-Ferreira J, Vilela J, Fonseca MM *et al.* (2014) The elusive nature of adaptive mitochondrial DNA evolution of an arctic lineage prone to frequent introgression. *Genome Biology and Evolution*, **6**, 886–896.

Muir G, Schlötterer C (2005) Evidence for shared ancestral polymorphism rather than recurrent gene flow at microsatellite loci differentiating two hybridizing oaks (*Quercus* spp.). *Molecular Ecology*, **14**, 549–561.

Nadachowska K, Babik W (2009) Divergence in the face of gene flow: the case of two newts (Amphibia: Salamandridae). *Molecular Biology and Evolution*, **26**, 829–841.

Nesi N, Nakoune E, Cruaud C, Hassanin A (2011) DNA barcoding of African fruit bats (Mammalia, Pteropodidae). The mitochondrial genome does not provide a reliable discrimination between *Epomophorus gambianus* and *Micropteropus pusillus*. *Comptes Rendus Biologies*, **334**, 544–554.

Nielsen R, Wakeley J (2001) Distinguishing migration from isolation: a Markov chain Monte Carlo approach. *Genetics*, **158**, 885–896.

Papadopulos AST, Baker WJ, Crayn D *et al.* (2011) Speciation with gene flow on Lord Howe Island. *Proceedings of the National Academy of Sciences of the USA*, **108**, 13188–13193.

Petit RJ, Excoffier L (2009) Gene flow and species delimitation. *Trends in Ecology & Evolution*, **24**, 386–393.

Phillimore AB, Orme CDL, Thomas GH *et al.* (2008) Sympatric speciation in birds is rare: insights from range data and simulations. *The American Naturalist*, **171**, 646–657.

Polzin T, Daneshmand SV (2003) On Steiner trees and minimum spanning trees in hypergraphs. *Operations Research Letters*, **31**, 12–20.

Posada D (2008) jModelTest: phylogenetic model averaging. *Molecular Biology and Evolution*, **25**, 1253–1256.

Pritchard JK, Stephens M, Donnelly P (2000) Inference of population structure using multilocus genotype data. *Genetics*, **155**, 945–959.

Rambaut A, Drummond AJ (2007) *Tracer v1.4*. Available from http://tree.bio.ed.ac.uk/software/tracer/.

Randi E (2008) Detecting hybridization between wild species and their domesticated relatives. *Molecular Ecology*, **17**, 285–293.

Rice WR (1984) Disruptive selection on habitat preference and the evolution of reproductive isolation—a simulation study. *Evolution*, **38**, 1251–1260.

Rosenberg NA (2004) DISTRUCT: a program for the graphical display of population structure. *Molecular Ecology Notes*, **4**, 137–138.

Rossiter SJ, Benda P, Dietz C, Zhang S, Jones G (2007) Range-wide phylogeography in the greater horseshoe bat inferred from microsatellites: implications for population history, taxonomy and conservation. *Molecular Ecology*, **16**, 4699–4714.

Schmieder DA, Kingston T, Hashim R, Siemers BM (2010) Breaking the trade-off: rainforest bats maximize bandwidth and repetition rate of echolocation calls as they approach prey. *Biology Letters*, **6**, 604–609.

Slatkin M (1982) Pleiotropy and parapatric speciation. *Evolution*, **36**, 263–270.

Stephens M, Scheet P (2005) Accounting for decay of linkage disequilibrium in haplotype inference and missing data imputation. *American Journal of Human Genetics*, **76**, 449–462.

Stephens M, Smith NJ, Donnelly P (2001) A new statistical method for haplotype reconstruction from population data. *American Journal of Human Genetics*, **68**, 978–989.

Strasburg JL, Rieseberg LH (2011) Interpreting the estimated timing of migration events between hybridizing species. *Molecular Ecology*, **20**, 2353–2366.

Struebig MJ, Kingston T, Petit EJ *et al.* (2011) Parallel declines in species and genetic diversity in tropical forest fragments. *Ecology Letters*, **14**, 582–590.

Tamura K, Peterson D, Peterson N *et al.* (2011) MEGA5: molecular evolutionary genetics analysis using maximum likelihood, evolutionary distance, and maximum parsimony methods. *Molecular Biology and Evolution*, **28**, 2731–2739.

Tavaré S (1986) Some probabilistic and statistical problems in the analysis of DNA sequences. In: *Some Mathematical Questions in Biology: DNA Sequence Analysis* (ed. Miura RM), pp. 57–86. American Mathematical Society, Providence, Rhode Island.

Toews DPL, Brelsford A (2012) The biogeography of mitochondrial and nuclear discordance in animals. *Molecular Ecology*, **21**, 3907–3930.

Turelli M, Barton NH, Coyne JA (2001) Theory and speciation. *Trends in Ecology & Evolution*, **16**, 330–343.

Vallo P, Benda P, Cerveny J, Koubek P (2013) Conflicting mitochondrial and nuclear paraphyly in small-sized West African house bats (Vespertilionidae). *Zoologica Scripta*, **42**, 1–12.
Via S (2001) Sympatric speciation in animals: the ugly duckling grows up. *Trends in Ecology & Evolution*, **16**, 381–390.
Voris HK (2000) Maps of Pleistocene sea levels in Southeast Asia: shorelines, river systems and time durations. *Journal of Biogeography*, **27**, 1153–1167.
Watterson GA (1975) On the number of segregating sites in genetical models without recombination. *Theoretical Population Biology*, **7**, 256–276.
White MJD (1978) *Modes of Speciation*. W. H. Freeman and Company, San Francisco, California.
Woerner AE, Cox MP, Hammer MF (2007) Recombination-filtered genomic datasets by information maximization. *Bioinformatics*, **23**, 1851–1853.
Yu HT (1995) Patterns of diversification and genetic population structure of small mammals in Taiwan. *Biological Journal of the Linnean Society*, **55**, 69–89.
Yule GU (1924) A mathematical theory of evolution based on the conclusions of Dr J. C. Willis. *Philosophical Transactions of the Royal Society of London B: Biological Sciences*, **213**, 21–87.

H.-C.K., S.-F.C., Y.-P.F., C.-H. Chen and C.-H. Chou collected tissue samples from Taiwanese taxa; G.C., B.K.L. and J.L.E. provided tissue samples of *M. eleryi*; H.-C.K. conducted laboratory work under the supervision of S.J.R., and performed statistical analyses with input from S.J.R., J.A.C. and J.D.P. H.-C.K. wrote the manuscript with S.J.R., and all authors participated in discussions.

Data accessibility

GenBank accessions for new *M. eleryi* sequences are KT762291–KT762293 for COI, KT762294–KT762306 for Cyt-*b* and KT778876–KT779034 (unphased) for microsatellite flanking regions. GenBank accessions for microsatellite flanking sequences of *M. gracilis* and *M. recondita* generated via 454-pyrosequencing are KT794560–KT795100. For all focal taxa studied, we created an archive comprising (i) alignments of phased sequences at two microsatellite flanking regions used to produce Fig. 2, (ii) an alignment of concatenated Cyt-*b* and COI genes used to produce Fig. 3a, (iii) alignments of phased sequences at 10 microsatellite flanking regions used to produce Fig. 3b and (iv) input data for the four-taxon IM analyses. This archive is accessible with the Dryad entry: doi: 10.5061/dryad.19923.

Supporting information

Additional supporting information may be found in the online version of this article.

Appendix S1 Materials and methods.

Fig. S1 Median-joining networks built for the *Murina gracilis* complex based on 10 microsatellite flanking regions.

Fig. S2 Marginal densities for demographic parameters from a four-taxon IM analysis of the *Murina gracilis* complex.

Fig. S3 Marginal densities for demographic parameters from IM analyses for the 6 two-taxon pairs of the *Murina gracilis* complex.

Fig. S4 A mitochondrial gene tree used in tests of positive selection.

Fig. S5 Samples of *Murina gracilis* and *Murina recondita* analysed for sex-biased dispersal.

Fig. S6 Correlograms of individual-level analyses of sex-biased dispersal in *Murina gracilis* and *Murina recondita*.

Table S1 External measurements showing body sizes of *Murina gracilis* and its relatives

Table S2 Details of 13 voucher specimens of *Murina eleryi* sampled for genetic analyses

Table S3 Primer pairs for amplification of flanking regions of 10 microsatellite loci

Table S4 Estimated proportions of 'foreign' genetic composition for four individual bats of *Murina recondita* as inferred from STRUCTURE analyses

Table S5 IM estimates based on all four taxa from the *Murina gracilis* complex

Table S6 IM estimates for six pairs of two taxa from the *Murina gracilis* complex

Table S7 Sources of mitochondrial sequences used in maximum-likelihood analyses in PAML to test for signatures of positive selection

Table S8 Predictions and results of the population-level tests—based on four statistics—for evidence of male-biased dispersal in *Murina gracilis* and *Murina recondita*